

## Enhanced NO<sub>2</sub> sensing performance of S-doped biomorphic SnO<sub>2</sub> with increased active-sites and charge transfer at room temperature

Wenna Li<sup>a</sup>, Lang He<sup>a</sup>, Xue Bai<sup>a</sup>, Lujia Liu<sup>a</sup>, Muhammad Ikram<sup>a</sup>, He Lv<sup>a</sup>, Mohib Ullah<sup>a</sup>, Mawaz Khan<sup>a</sup>, Kan Kan<sup>\*b</sup>, and Keying Shi<sup>\*a</sup>

<sup>a</sup>Key Laboratory of Functional Inorganic Material Chemistry, Ministry of Education, School of Chemistry and Material Science, Heilongjiang University, Harbin, 150080, P. R. China. E-mail:  
*shikeying2008@163.com*

<sup>b</sup>Heilongjiang Academy of Sciences, Institute of Advanced Technology, Harbin 150020, P. R. China. E-mail: *kankan.has@foxmail.com*

### \*Corresponding authors:

<sup>a</sup> Key Laboratory of Functional Inorganic Material Chemistry, Ministry of Education, School of Chemistry and Material Science, Heilongjiang University, Harbin 150080, P. R. China. E-mail:  
*shikeying2008@163.com*

<sup>b</sup> Heilongjiang Academy of Sciences, Institute of Advanced Technology, Harbin 150020, China. E-mail: *kankan.has@foxmail.com*

## **Table of Contents for Supporting Information**

1. Fig. S1. SEM of S-BCS-500 and S-BCS-700	Page S3
2. Fig. S2. The BET of S-BCS-500 and S-BCS-700	Page S3
3. Fig. S3. DRIFT spectra of S-BCS-600	Page S4
4. Fig. S4. Gas sensing dynamic curves of S-BCS-500 and S-BCS-700	Page S4
5. Fig. S5. Sensitivity of S-BCS and BCS-450 and the calibration curve of S-BCS-600	Page S5
6. Fig. S6. XPS of fresh S-BCS-600 and used sample: Sn 3d and O 1s	Page S5
7. Table S1. Sn 3d <sub>5/2</sub> peaks position and peak area ratio (%) of three series of samples	Page S5
8. Table S2. O 1s peaks position and peak area ratio (%) of three series of samples	Page S5
9. Table S3. Comparison of related works towards NO <sub>2</sub> and other gases	Page S6
10. Table S4. S-BCS-500, S-BCS -600 and S-BCS-700 gas sensing performance to NO <sub>2</sub>	Page S6
11. Reference	Page S7

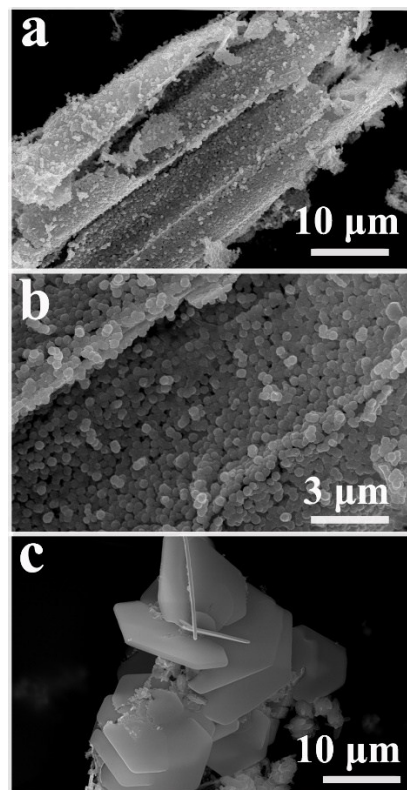


**Fig. S1** (a) SEM of S-BCS-500; (b) Enlarge SEM of (a) shows the morphology of S-BCS-500; (c) SEM of S-BCS-  
700.

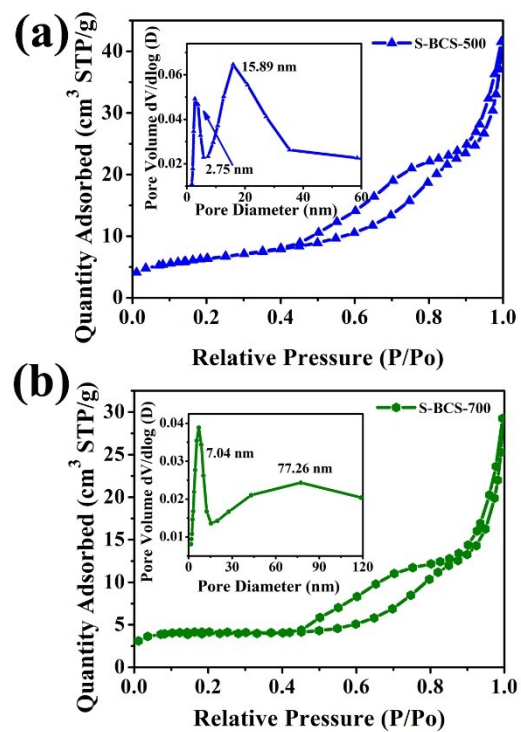


**Fig. S2** The  $\text{N}_2$  adsorption-desorption isotherms and pore size distribution (inset) of: (a) S-BCS-500; (b) S-BCS-700

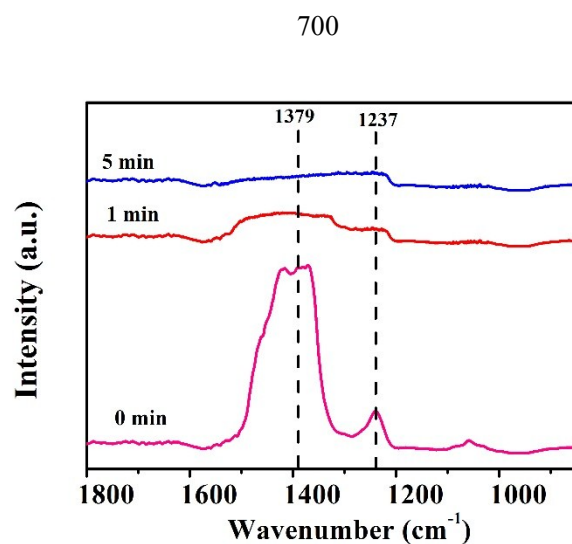


**Fig. S3** DRIFT spectra of S-BCS-600 by passing  $\text{NO}_2$  gases at 30 °C for 5 min, then purge by  $\text{N}_2$  at 30 °C.

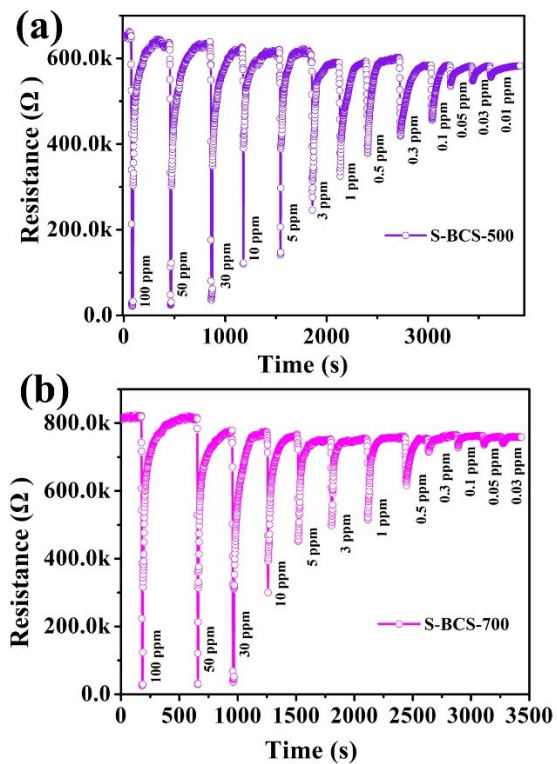


**Fig. S4** Dynamic response-recovery curve and response time of the (a) S-BCS-500; (b) S-BCS-700 sensor to 100-0.01 ppm  $\text{NO}_2$  gas at the RT (RH 26%).

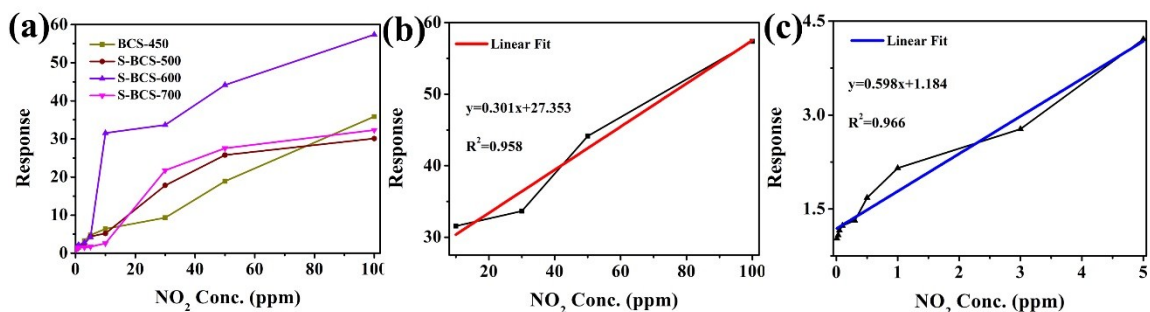


**Fig. S5** (a) Response of S-BCS series samples and BCS-450 to 100 ~ 0.01 ppm  $\text{NO}_2$  at RT; the calibration curve of S-BCS-600: (b) 100 ~ 10 ppm  $\text{NO}_2$ ; (c) 5 ~ 0.01 ppm  $\text{NO}_2$ .

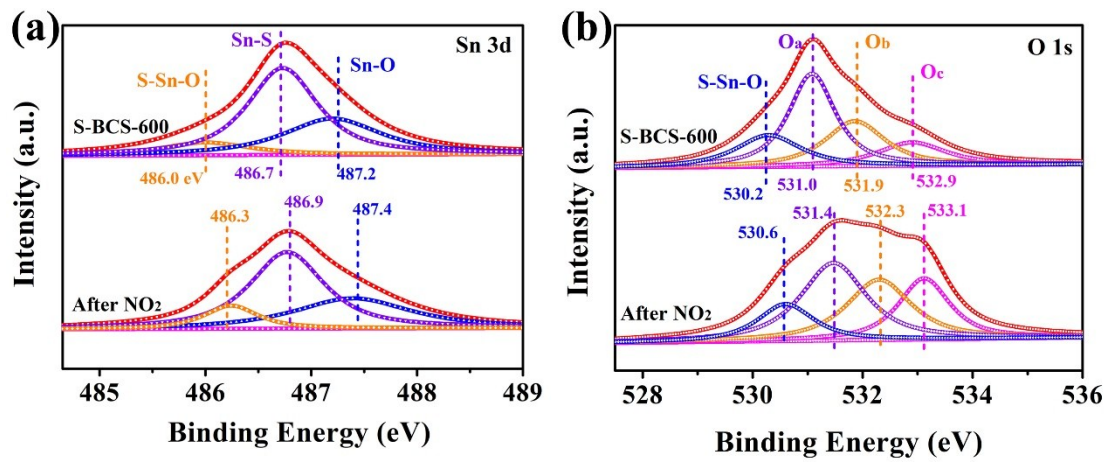


**Fig. S6** XPS of fresh S-BCS-600 and used sample: (a) Sn; (b) O 1s (used sample: contacted with NO<sub>2</sub> for 1 h)

**Table S1.** Sn 3d<sub>5/2</sub> peaks position and peak area ratio (%) of three series of samples

Sample	S-BCS-500			S-BCS-600			S-BCS-700		
Chemical Bonds	Sn-O	Sn-S	S-Sn-O	Sn-O	Sn-S	S-Sn-O	Sn-O	Sn-S	S-Sn-O
Peak position(eV)	487.2	-	-	487.2	486.7	486.0	487.2	486.7	486.0
Peak area ratio (%)	100	-	-	32.8	56.5	10.7	30.9	62.7	6.4

**Table S2.** O 1s peaks position and peak area ratio (%) of three series of samples

Sample	S-BCS-500			S-BCS-600			S-BCS-700				
Chemical Bonds	O <sub>a</sub>	O <sub>b</sub>	O <sub>c</sub>	O <sub>a</sub>	O <sub>b</sub>	O <sub>c</sub>	S-Sn-O	O <sub>a</sub>	O <sub>b</sub>	O <sub>c</sub>	S-Sn-O
Peak position(eV)	531.0	531.9	532.9	531.0	531.9	532.9	530.2	531.0	531.9	532.9	530.2
Peak area ratio (%)	48.1	30.1	21.8	40.4	25.3	15.0	19.3	21.3	37.8	26.9	14.0

**Table S3.** Comparison of the sensing performances of SnO<sub>2</sub>-based gas sensors and SnS<sub>2</sub>-based gas sensors towards NO<sub>2</sub> and other gases

Composite	Method	Target gas	Temperature (°C)	Response	Detection Limit	Reference
SnO <sub>2</sub> -SnS <sub>2</sub>	Oxidation method	NH <sub>3</sub> (10 ppm)	RT	1.16	10 ppm	1
SnS <sub>2</sub>	CVD system	NO <sub>2</sub> (10 ppm)	RT	701%	408.9 ppb	2
SnS <sub>2</sub>	wet chemical route	NO <sub>2</sub> (10 ppm)	120	36	1 ppm	3
SnO <sub>2</sub> -SnS <sub>2</sub>	Oxidation method	NO <sub>2</sub> (5 ppm)	50	600	50 ppb	4
SnO <sub>2</sub> -SnS <sub>2</sub>	Microwave method	NO <sub>2</sub> (1 ppm)	100	51.1	125 ppb	5

SnO <sub>2</sub> -SnS <sub>2</sub>	Oxidation method	NO <sub>2</sub> (8 ppm)	80	5.3	1 ppm	6
SnS <sub>2</sub>	Chemical exfoliation	NO <sub>2</sub> (100 ppm)	RT	2.31	20 ppm	7
SnS <sub>2</sub> -reduced graphene	Wet chemical method	NO <sub>2</sub> (11.9 ppm)	80	56.8%	0.6 ppm	8
SnS <sub>2</sub>	Hydrothermal method	NO <sub>2</sub> (0.5 ppm)	120	25.4	couple of tens of ppb	9
S-doped biomorphic SnO <sub>2</sub>	CVD system	NO <sub>2</sub> (100 ppm)	RT	57.38	10 ppb	This work

**Table S4.** Response (R), response time (T<sub>1</sub>) and recovery time (T<sub>2</sub>) of S-BCS-500, S-BCS-600 and S-BCS-700 to

NO<sub>2</sub> at RT.

Sample	S-BCS-500			S-BCS-600			S-BCS-700			
	NO <sub>2</sub> /ppm	R	T <sub>1</sub> /s	T <sub>2</sub> /s	R	T <sub>1</sub> /s	T <sub>2</sub> /s	R	T <sub>1</sub> /s	T <sub>2</sub> /s
100	30.10	5.33	68.80	57.38	1.60	53.87	32.34	5.33	71.47	
50	25.76	6.93	73.07	44.14	3.73	54.93	27.57	3.20	77.87	
30	17.78	6.93	78.40	33.66	4.27	60.27	21.74	5.33	78.40	
10	5.17	5.33	84.27	31.56	4.80	62.93	2.58	5.87	73.60	
5	4.40	5.87	85.33	4.21	5.87	61.33	1.70	5.33	76.27	
3	2.48	7.47	91.20	2.78	5.87	61.87	1.51	3.73	80.07	
1	1.82	5.87	89.07	2.15	6.93	62.93	1.46	3.73	86.40	
0.5	1.57	7.47	97.60	1.68	6.93	67.20	1.23	6.40	84.67	
0.3	1.43	6.40	97.07	1.31	6.93	68.27	1.05	3.73	90.80	
0.1	1.28	5.87	89.60	1.23	7.46	68.80	1.05	4.27	94.13	
0.05	1.09	3.73	85.87	1.16	7.46	70.40	1.04	6.93	92.20	
0.03	1.06	5.33	84.80	1.08	8.53	74.13	1.03	8.00	90.93	
0.01	1.05	5.87	140.80	1.03	13.87	76.80				

## Reference

- 1 K. Xu, N. Li, D. Zeng, S. Tian, S. Zhang, D. Hu and C. Xie, Interface Bonds Determined Gas-Sensing of SnO<sub>2</sub>-SnS<sub>2</sub> Hybrids to Ammonia at Room Temperature, *ACS Appl Mater Interfaces*, 2015, **7**, 11359-11368.
- 2 K. C. Kwon, J. M. Suh, T. H. Lee, K. S. Choi, K. Hong, Y. G. Song, Y. S. Shim, M. Shokouhimehr, C. Y. Kang, S. Y. Kim and H. W. Jang, SnS<sub>2</sub> Nanograins on Porous SiO<sub>2</sub> Nanorods Template for Highly Sensitive NO<sub>2</sub> Sensor at Room Temperature with Excellent Recovery, *ACS Sens*, 2019, **4**, 678-686.
3. J. Z. Ou, W. Ge, B. Carey, T. Daeneke, A. Rotbart, W. Shan, Y. Wang, Z. Fu, A. Chrimes and W. Wlodarski, Physisorption Based Charge Transfer in Two-Dimensional SnS<sub>2</sub> for Selective and Reversible NO<sub>2</sub> Gas Sensing.
- 4 K. Xu, S. Tian, J. Zhu, Y. Yang, J. Shi, T. Yu and C. Yuan, High selectivity of sulfur-doped SnO<sub>2</sub> in NO<sub>2</sub> detection at lower operating temperatures, *Nanoscale*, 2018, **10**, 20761-20771.
- 5 J. Hao, D. Zhang, Q. Sun, S. Zheng, J. Sun and Y. Wang, Hierarchical SnS<sub>2</sub>/SnO<sub>2</sub> nanoheterojunctions with increased active-sites and charge transfer for ultrasensitive NO<sub>2</sub> detection, *Nanoscale*, 2018, **10**, 7210-7217.
- 6 D. Gu, X. Li, Y. Zhao and J. Wang, Enhanced NO<sub>2</sub> sensing of SnO<sub>2</sub>/SnS<sub>2</sub> heterojunction based sensor, *Sensors and*

*Actuators B: Chemical*, 2017, **244**, 67-76.

7 Z. Qin, K. Xu, H. Yue, H. Wang, J. Zhang, C. Ouyang, C. Xie and D. Zeng, Enhanced room-temperature NH<sub>3</sub> gas sensing by 2D SnS<sub>2</sub> with sulfur vacancies synthesized by chemical exfoliation, *Sensors and Actuators B: Chemical*, 2018, **262**, 771-779.

8 M. Shafiei, J. Bradford, H. Khan, C. Piloto, W. Wlodarski, Y. Li and N. Motta, Low-operating temperature NO<sub>2</sub> gas sensors based on hybrid two-dimensional SnS<sub>2</sub>-reduced graphene oxide, *Applied Surface Science*, 2018, **462**, 330-336.

9 D. Liu, Z. Tang and Z. Zhang, Nanoplates-assembled SnS<sub>2</sub> nanoflowers for ultrasensitive ppb-level NO<sub>2</sub> detection, *Sensors and Actuators B: Chemical*, 2018, **273**, 473-479.